Supporting Information

Stepwise bulk-to-cluster-to-particle transformation toward efficient synthesis of alkynyl-protected silver nanoclusters

Hui Guo,[a,b] Xin He,[b] Chong-Qing Wan,[a,*] and Liang Zhao[b,*]

[a] *Beijing Key Laboratory for Optical Materials and Photonic Devices, Department of Chemistry, Capital Normal University, Beijing 100048, China.*

E-mail: wancq@cnu.edu.cn

[b] *Key Laboratory of Bioorganic Phosphorus Chemistry & Chemical Biology (Ministry of Education), Department of Chemistry, Tsinghua University, Beijing 100084, China.*

E-mail: zhaolchem@mail.tsinghua.edu.cn

Synthesis

All commercially available chemicals were used without further purification. Methylazacalix[6]pyridine (**Py[6]**) was synthesized according to the literature method by the [3+3] fragment coupling protocol between terminal dibrominated and diaminated linear trimers.[1] **1a-f** were synthesized according to the literature.[2-4] The solvents used in this study were processed by standard procedures. ^{1}H-NMR experiments were carried out on a JEOL ECX-400MHz instrument.

Synthesis of [Ag_3(*p*-$MeOC_6H_4C{\equiv}C$)(Py[6])](CF_3SO_3)$_2$ (2a). In a 5 mL glass vial, $AgSO_3CF_3$ (25.7 mg, 0.1 mmol) was dissolved in CH_3OH (1 ml) at room temperature. Then [*p*-$MeOC_6H_4C{\equiv}CAg$] (**1a**, 11.9 mg, 0.05 mmol) solid was added to the solution under stirring. After 5 min, a CH_2Cl_2 solution (1 mL) of methylazacalix[6]pyridine (**Py[6]**, 6.4 mg, 0.01 mmol) was added dropwisely. The mixture was further stirred for 2 hours at room temperature. The solution was filtered and the filtrate was diffused by diethyl ether in the dark. After several days, pale yellow crystals of **2a** were deposited.

Synthesis of 2b-f. The synthesis of complexes **2b-f** is identical with the synthetic method for **2a** but with other substituted silver phenylacetylides **1b-f** in place of **1a**.

Preparation of 2d-NP. In a 10 mL glass vial, HPF_6 (0.2 mmol) was added dropwisely to the solution of **2d** (0.8 g/L, 3.5 mL). The solution was centrifuged to give the solid sample of **2d-NP**. This sample was washed three times by ethanol and was then dispersed in toluene for TEM and UV-vis studies.

Preparation of 2d-Ag-NC. In a 10 mL glass vials, HPF_6 (0.2 mmol) was added dropwisely to the solution of **2d** (0.8 g/L), respectively. The solution was centrifuged to give a solid sample of **2d-NP**. The solid sample was washed three times by ethanol and was then dispersed in toluene. Then $NaBH_4$ (0.01 mmol, in ethanol) was added dropwisely to the solution of **2d-NP** at 0 °C. The solution was centrifuged to give the solid sample of **2d-Ag-NC**. This solid was washed three times by ethanol and was dispersed in toluene for TEM and UV-vis studies.

X-ray crystallographic analysis

Data for complex **2a** (CCDC-1441335) was collected at 296K with Mo-$K\alpha$ radiation (λ = 0.71073 Å) on a Bruker APEXII CCD diffractometer with frames of oscillation range 0.5°. All structures were solved by direct methods, and non-hydrogen atoms were located from difference Fourier maps. All non-hydrogen atoms were subjected to anisotropic refinement by full-matrix least-squares on F^2 by using the SHELXTL program unless otherwise noticed.[5]

Crystal data for **$[Ag_3(p\text{-}MeOC_6H_4C{\equiv}C)(Py[6])](CF_3SO_3)_2$ (2a)**: $C_{47}H_{43}Ag_3F_6N_{12}O_7S_2$, M = 1389.66, triclinic, space group P-1, a = 12.88 (3) Å, b = 13.13(4) Å, c = 15.88(4) Å, α = 99.38(2), β = 90.29(3), γ = 101.76(6) , V = 2593(12) Å^3, Z = 2, T = 296(2) K, D_c = 1.780 g/cm^{-3}. The structure, refined on F^2, converged for 12200 unique reflections (R_{int} = 0.0373) and 9286 observed reflections with $I > 2\sigma(I)$ to give R_1 = 0.0450 and wR_2 = 0.1179 and a goodness-of-fit = 1.033.

Bond distances (Å) and angles (°) of 2a:

Ag1-C37	2.143(6)	Ag3-C37	2.297(6)
Ag1-N9	2.255(5)	Ag3-N5	2.333(6)
Ag1-Ag2	3.195(6)	Ag3-C38	2.429(6)
Ag2-C37	2.123(6)	Ag3-C10	2.574(7)
Ag2-N1	2.252(5)	Ag3-C20	2.676(6)
Ag2-Ag3	3.356(9)	N7-C23	1.350(5)
N1-C1	1.357(6)	N7-C19	1.351(6)
N1-C5	1.363(6)	C19-C20	1.406(6)
C1-C2	1.395(6)	C20-C21	1.402(6)
C1-N12	1.420(6)	C21-C22	1.392(7)
C2-C3	1.392(7)	C22-C23	1.407(6)
C3-C4	1.385(7)	C23-N8	1.409(6)
C4-C5	1.395(6)	N8-C25	1.419(6)
C5-N2	1.412(6)	N8-C24	1.471(6)
N2-C7	1.402(6)	N9-C25	1.361(6)
N2-C6	1.475(6)	N9-C29	1.367(5)
N3-C11	1.348(6)	C25-C26	1.403(6)
N3-C7	1.359(6)	C26-C27	1.400(7)
C7-C8	1.407(7)	C27-C28	1.363(7)
C8-C9	1.379(7)	C28-C29	1.400(6)
C9-C10	1.401(6)	C29-N10	1.400(6)
C10-C11	1.413(7)	N10-C31	1.414(6)
C11-N4	1.411(6)	N10-C30	1.485(6)
N4-C13	1.408(6)	N11-C31	1.345(6)
N4-C12	1.477(7)	N11-C35	1.358(6)
N5-C17	1.360(6)	C31-C32	1.412(7)
N5-C13	1.362(6)	C32-C33	1.392(7)
C13-C14	1.402(6)	C33-C34	1.394(6)
C14-C15	1.384(7)	C34-C35	1.404(7)
C15-C16	1.382(7)	C35-N12	1.400(6)
C16-C17	1.401(6)	N12-C36	1.473(6)
C17-N6	1.410(6)	O1-C42	1.375(5)
N6-C19	1.412(5)	O1-C45	1.442(7)
N6-C18	1.480(6)	C37-C38	1.236(6)
S1-O3	1.431(5)	C38-C39	1.454(6)
S1-O2	1.435(5)	C39-C40	1.396(6)
S1-O4	1.440(5)	C39-C44	1.400(7)
S1-C46	1.822(6)	C40-C41	1.390(6)
F11-C46	1.337(7)	C41-C42	1.389(7)
F12-C46	1.328(6)	C42-C43	1.395(7)
F13-C46	1.344(7)	C43-C44	1.386(7)

S2-O5	1.435(5)	F21-C47	1.324(7)
S2-O6	1.439(5)	F22-C47	1.367(9)
S2-O7	1.446(4)	F23-C47	1.336(8)
S2-C47	1.806(8)		

C37- Ag1- N9	164.16(13)	N10- C29- C28	121.9(4)
C37- Ag1- Ag2	41.26(13)	C29- N10- C31	122.6(3)
N9- Ag1- Ag2	154.57(10)	C29- N10- C30	118.5(4)
C37- Ag2- N1	174.98(14)	C31- N10- C30	118.9(4)
C37- Ag2- Ag1	41.76(13)	C31- N11- C35	118.4(4)
N1- Ag2- Ag1	140.07(13)	N11- C31- C32	122.8(4)
C37- Ag2- Ag3	42.57(16)	N11- C31- N10	115.8(4)
N1- Ag2- Ag3	132.45(16)	C32- C31- N10	121.3(4)
Ag1- Ag2- Ag3	65.04(14)	C33- C32- C31	117.4(4)
C37- Ag3- N5	142.81(17)	C32- C33- C34	121.0(4)
C37- Ag3- C38	30.16(14)	C33- C34- C35	117.3(4)
N5- Ag3- C38	112.85(19)	N11- C35- N12	115.4(4)
C37- Ag3- C10	133.46(18)	N11- C35- C34	123.0(4)
N5- Ag3- C10	73.93(18)	N12- C35- C34	121.7(4)
C38- Ag3- C10	149.16(14)	C35- N12- C1	121.5(4)
C37- Ag3- C20	124.75(18)	C35- N12- C36	120.0(4)
N5- Ag3- C20	73.6(2)	C1- N12- C36	117.5(4)
C38- Ag3- C20	125.38(18)	C42- O1- C45	117.0(4)
C10- Ag3- C20	85.44(18)	C38- C37- Ag2	141.5(3)
C37- Ag3- Ag2	38.69(12)	C38- C37- Ag1	120.5(3)
N5- Ag3- Ag2	151.49(11)	Ag2- C37- Ag1	96.98(19)
C38- Ag3- Ag2	64.48(11)	C38- C37- Ag3	80.9(3)
C10- Ag3- Ag2	94.85(12)	Ag2- C37- Ag3	98.7(2)
C20- Ag3- Ag2	132.66(14)	Ag1- C37- Ag3	105.0(2)
C1- N1- C5	118.8(3)	C37- C38- C39	177.7(4)
C1- N1- Ag2	118.5(3)	C37- C38- Ag3	69.0(3)
C5- N1- Ag2	121.3(3)	C39- C38- Ag3	112.1(3)
N1- C1- C2	122.1(4)	C40- C39- C44	118.6(4)
N1- C1- N12	117.8(3)	C40- C39- C38	120.4(4)
C2- C1- N12	120.1(4)	C44- C39- C38	121.1(4)
C3- C2- C1	118.7(4)	C41- C40- C39	121.2(4)
C4- C3- C2	119.6(4)	C42- C41- C40	119.4(4)
C3- C4- C5	119.3(5)	O1- C42- C41	123.8(4)
N1- C5- C4	121.5(4)	O1- C42- C43	116.1(4)
N1- C5- N2	117.9(3)	C41- C42- C43	120.1(4)
C4- C5- N2	120.6(4)	C44- C43- C42	120.1(4)
C7- N2- C5	121.9(4)	C43- C44- C39	120.5(4)

C7- N2- C6	119.2(4)	O3- S1- O2	115.0(3)
C5- N2- C6	118.8(4)	O3- S1- O4	114.2(3)
C11- N3- C7	118.0(4)	O2- S1- O4	115.6(3)
N3- C7- N2	115.0(4)	O3- S1- C46	104.6(3)
N3- C7- C8	122.7(4)	O2- S1- C46	102.4(3)
N2- C7- C8	122.2(4)	O4- S1- C46	102.7(3)
C9- C8- C7	118.3(4)	F12- C46- F11	106.0(5)
C8- C9- C10	120.4(4)	F12- C46- F13	108.8(5)
C9- C10- C11	117.4(4)	F11- C46- F13	106.8(4)
C9- C10- Ag3	97.6(3)	F12- C46- S1	112.6(4)
C11- C10- Ag3	80.8(3)	F11- C46- S1	112.0(4)
N3- C11- N4	114.9(4)	F13- C46- S1	110.4(4)
N3- C11- C10	123.1(4)	O5- S2- O6	113.5(3)
N4- C11- C10	122.0(4)	O5- S2- O7	114.8(3)
C13- N4- C11	123.6(4)	O6- S2- O7	116.0(3)
C13- N4- C12	118.0(4)	O5- S2- C47	103.8(4)
C11- N4- C12	118.2(4)	O6- S2- C47	102.8(3)
C17- N5- C13	119.1(3)	O7- S2- C47	103.6(3)
C17- N5- Ag3	122.2(3)	F21- C47- F23	107.9(6)
C13- N5- Ag3	117.8(3)	F21- C47- F22	107.6(6)
N5- C13- C14	121.7(4)	F23- C47- F22	107.7(6)
N5- C13- N4	118.5(3)	F21- C47- S2	111.7(5)
C14- C13- N4	119.6(4)	F23- C47- S2	111.3(5)
C15- C14- C13	118.1(4)	F22- C47- S2	110.5(5)
C16- C15- C14	120.9(4)	N7- C23- C22	122.1(4)
C15- C16- C17	118.5(4)	N7- C23- N8	115.1(4)
N5- C17- C16	121.5(4)	C22- C23- N8	122.8(3)
N5- C17- N6	118.1(3)	C23- N8- C25	123.2(3)
C16- C17- N6	120.1(4)	C23- N8- C24	117.9(4)
C17- N6- C19	124.0(3)	C25- N8- C24	118.7(4)
C17- N6- C18	117.6(3)	C25- N9- C29	118.6(4)
C19- N6- C18	118.3(4)	C25- N9- Ag1	119.7(2)
C23- N7- C19	119.5(3)	C29- N9- Ag1	120.7(3)
N7- C19- C20	122.4(4)	N9- C25- C26	121.9(4)
N7- C19- N6	115.4(4)	N9- C25- N8	117.4(4)
C20- C19- N6	122.1(4)	C26- C25- N8	120.5(4)
C21- C20- C19	117.1(4)	C27- C26- C25	118.1(4)
C21- C20- Ag3	96.5(3)	C28- C27- C26	120.3(4)
C19- C20- Ag3	81.7(3)	C27- C28- C29	119.4(4)
C22- C21- C20	121.1(4)	N9- C29- N10	116.5(4)
C21- C22- C23	117.6(4)	N9- C29- C28	121.5(4)

TEM Characterization

The morphology and size distribution of as-prepared Ag nanoparticles and nanoclusters was determined on a Hitachi H-7650 transmission electron microscope. The EDX and trials for searching lattice fringe of **2d-NP** were taken by a JEOL JEM-2011 and a FEI Tecnai G^2 20 high-resolution transmission electron microscope.

The yield determining of 2b-f-Ag-NC. In five 50 mL round-bottom flasks, **2b-f** (0.01 mmol, $[Ag_3(p\text{-}C_nH_{2n+1}OC_6H_4C{\equiv}C)(\mathbf{Py[6]})](CF_3SO_3)_2$, n=8, 10, 12, 14, 16) was dissolved in CH_3OH/CH_2Cl_2 (10 ml/10 ml) at room temperature, respectively. HPF_6 (0.2 mmol) was added dropwisely to the solutions of **2b-f**, respectively. The solutions were centrifuged to give solid samples, which were washed three times by ethanol and were dispersed in toluene. Then $NaBH_4$ (0.01 mmol, in ethanol) was added dropwisely to the solutions of **2b-f-NP** at 0 °C. The solutions were centrifuged to give solid samples of **2b-f-Ag-NC**. The solid samples were washed three times by ethanol. The dry solid samples each was respectively added in a solution of HNO_3 (16 mol/L, 2 mL). The resulting solutions were titrated by an aqueous solution of NaCl (0.1 mmol, 10 mL) to produce AgCl. The solids of AgCl were collected, washed and dried to measure their weight. The mass of acquired AgCl were 4.1 mg, 3.9 mg, 4.0 mg, 3.9 mg, 3.8 mg for **2b-f**, respectively. Then the yields of **2b-f-Ag-NC** were calculated as 95%, 91%, 93%, 91%, 88%, respectively.

References

[1] E.-X. Zhang, D.-X. Wang, Q.-Y. Zheng, M.-X. Wang, *Org. Lett.*, **2008**, *10*, 2565.

[2] A. Ikeda, M. Omote, K. Kusumoto, A. Tarui, K. Sato, A. Ando, *Org. Biomol. Chem.*, **2015**, *13*, 8886.

[3] S.-J. Lee, C.-R. Park, J.-Y. Chang, *Langmuir*, **2004**, *20*, 9513.

[4] C.-Y. Gao, L. Zhao and M.-X. Wang, *J. Am. Chem. Soc.,* **2012**, *134*, 824.

[5] a) G. M. Sheldrick, SHELXS-97 (Univ. Göttingen, 1990). b) G. M. Sheldrick, SHELXL-97 (Univ. Göttingen, 1997).

Supporting Figures

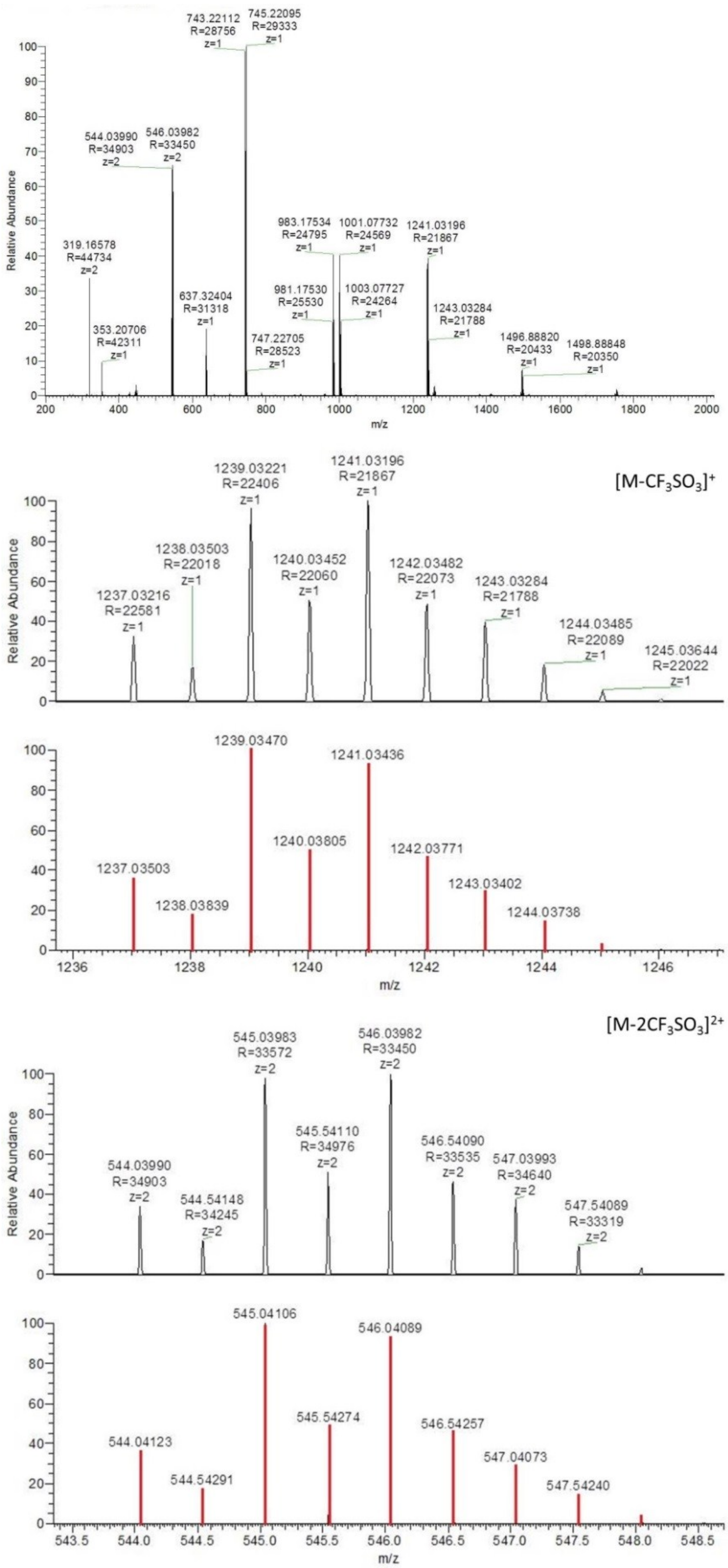

Figure S1. Electrospray ionization mass spectroscopy (ESI-MS) of complex **2a**. [M-CF_3SO_3]$^+$: 1241.0320, [M-2CF_3SO_3]$^{2+}$: 546.0398.

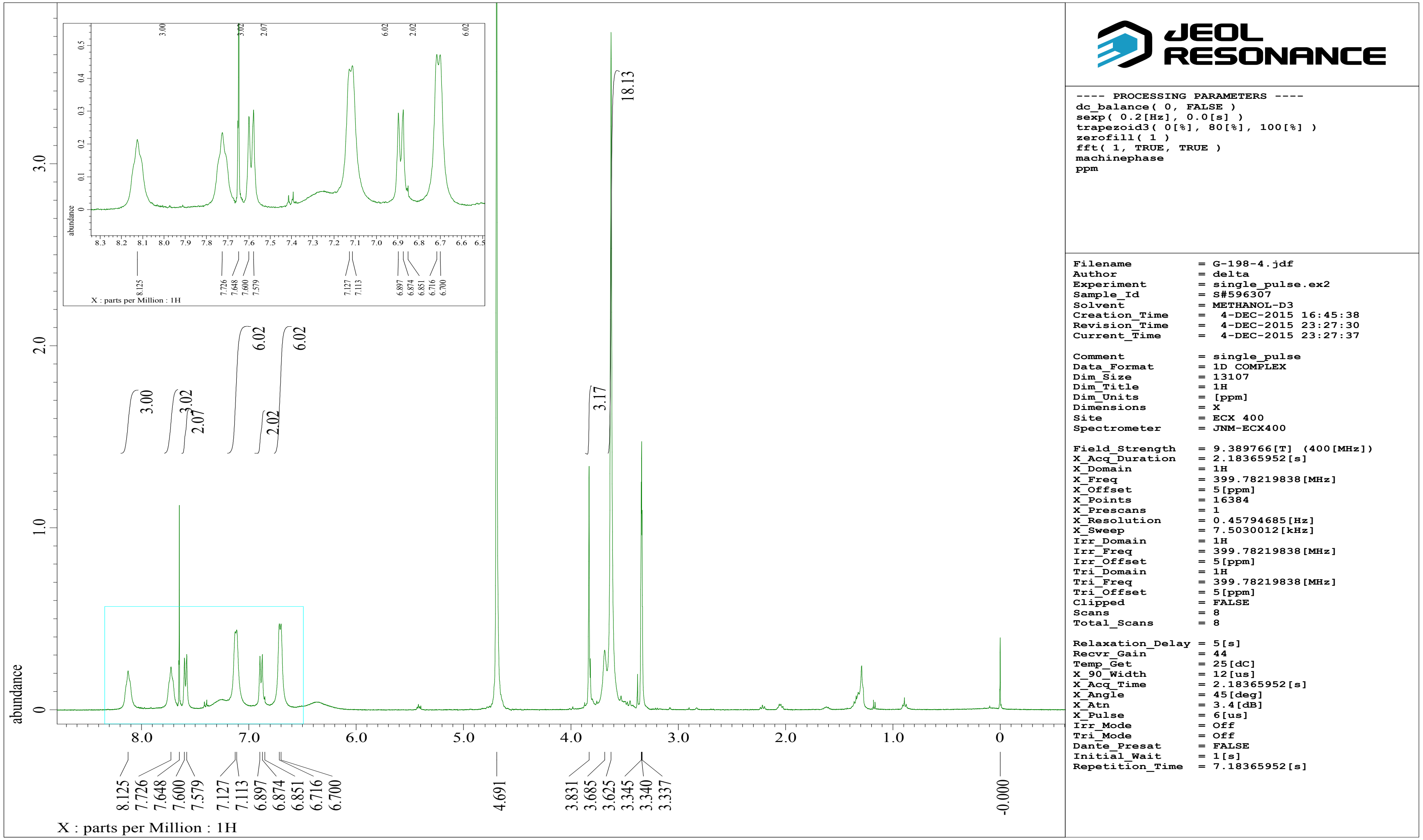

Figure S2. [1]H-NMR spectrum (400MHz, methanol-d_4:$CDCl_3$, v/v = 1:1) of **2a**.

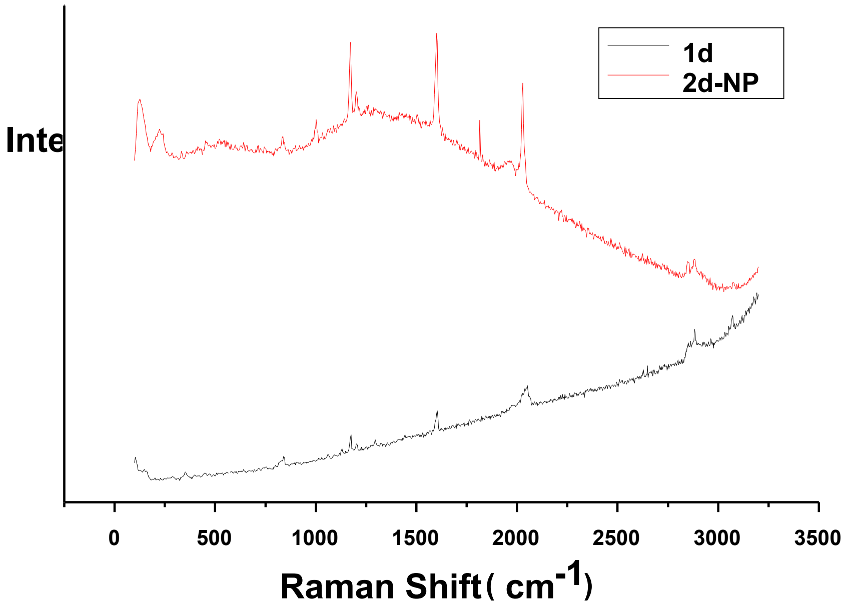

Figure S3. Raman spectrum of **1d** and **2d-NP**. The raman shift of C≡C in **1d** is 2047 cm^{-1} but 2029 cm^{-1}in **2d-NP**.

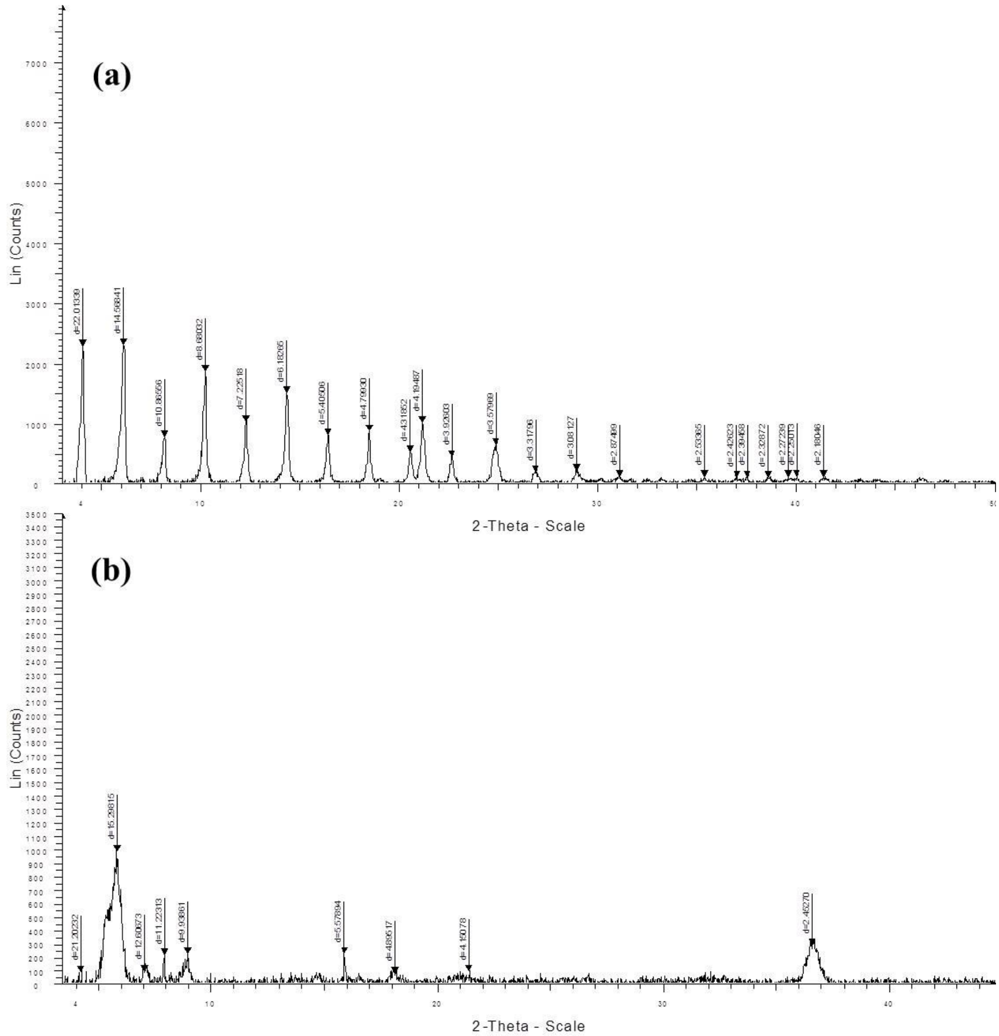

Figure S4. Powder X-ray diffraction (PXRD) of (a) **1d** and (b) **2d-NP**.

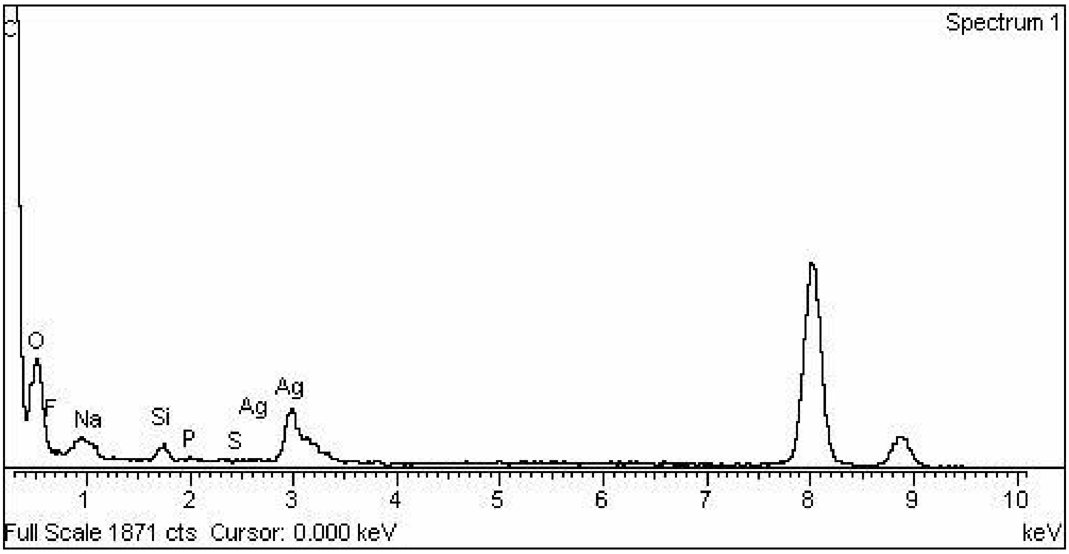

Figure S5. Energy dispersive X-ray spectroscopy (EDX) of **2d-NP**, suggesting the presence of the elements Ag, C, O, F, S and P.

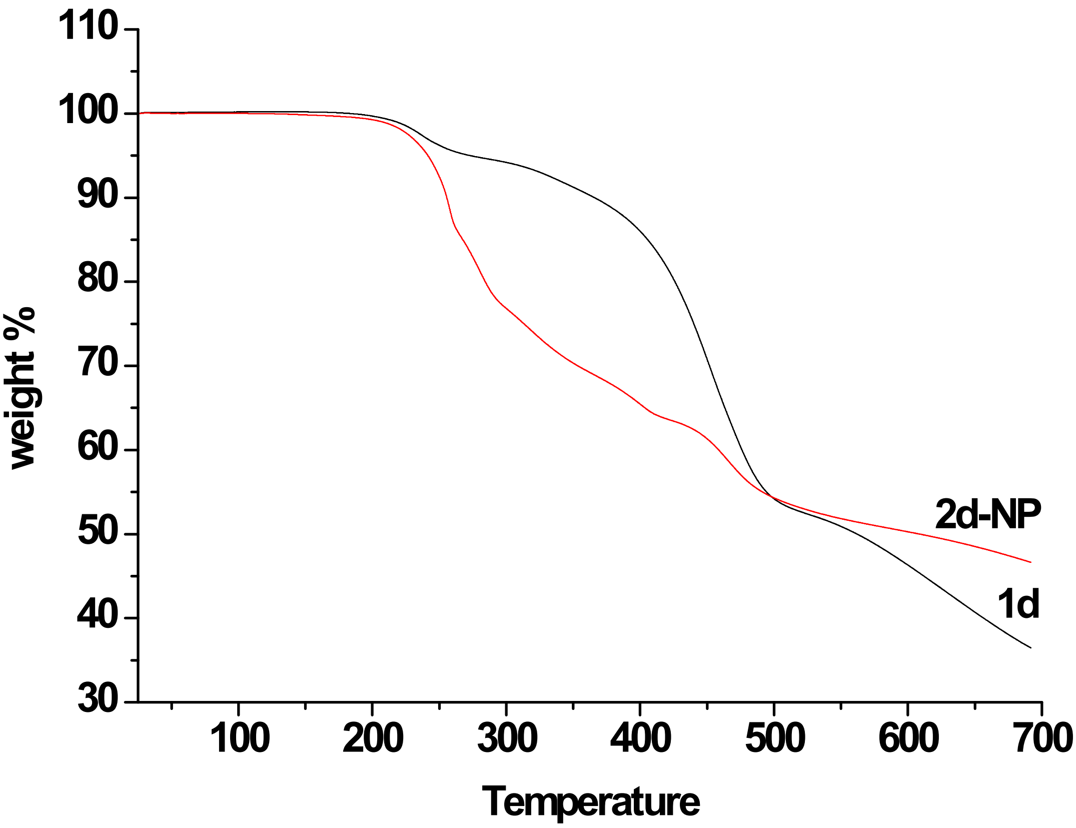

Figure S6. Thermal gravimetric analysis (TGA) of **1d** and **2d-NP**.

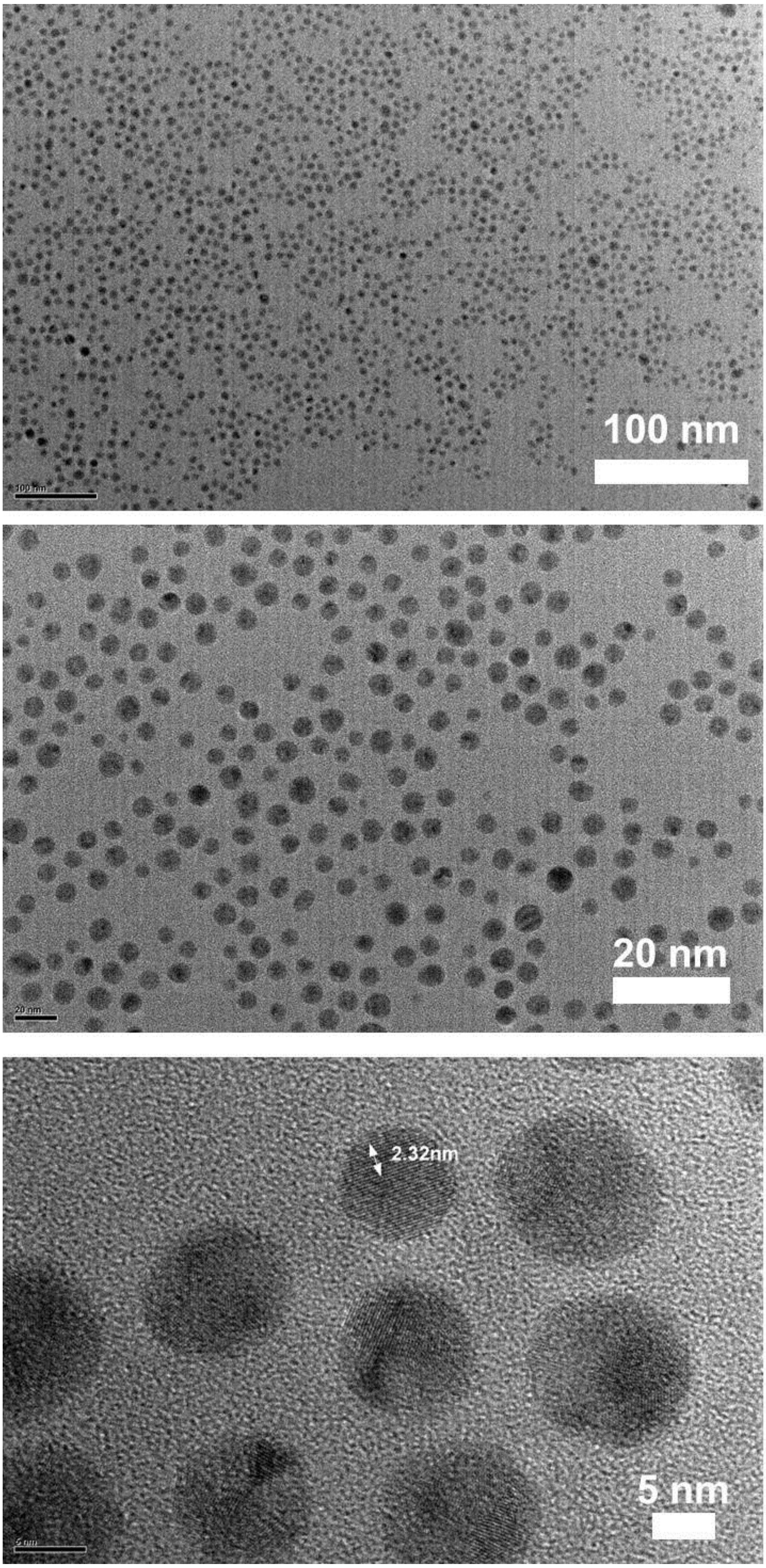

Figure S7. High-resolution TEM of **2d-NP**.

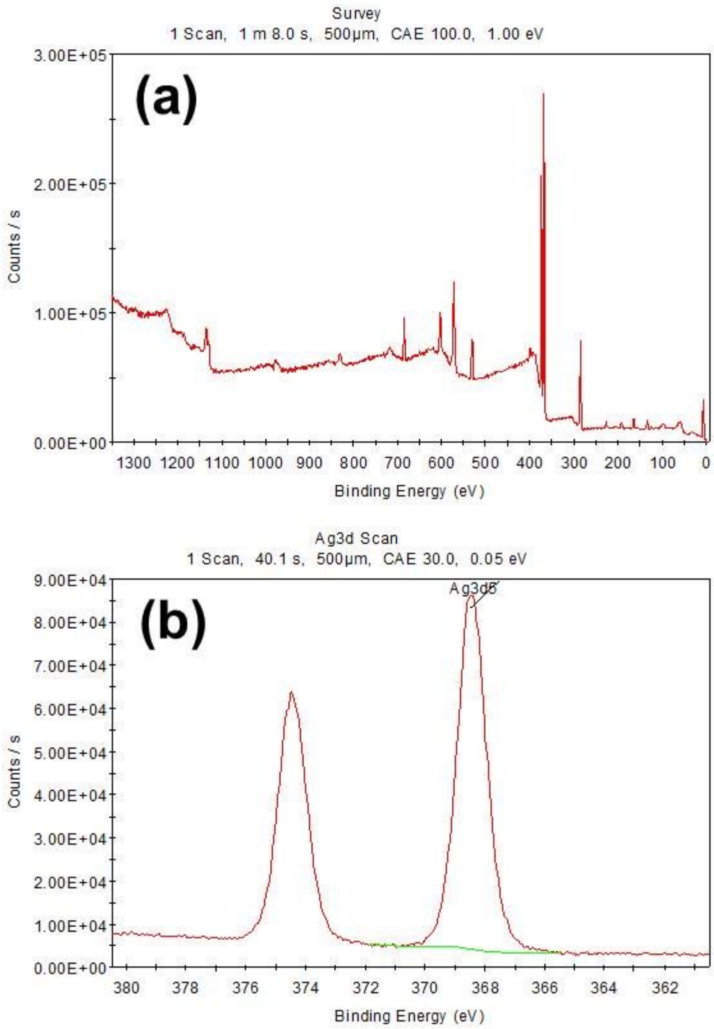

Name	**Start BE**	**Peak BE**	**End BE**	**Height CPS**	**FWHM eV**	**Area (P) CPS.eV**	**Area (N) TPP-2M**	**Atomic %**
Ag3d5	371.32	368.15	364.79	82452.95	1.1	102380.28	0.1	13.09
P2p	140.07	133.41	129.42	1425.41	1.97	3742.1	0.03	4.32
S2p	171.22	161.51	158.17	2348.52	1.15	3959.11	0.03	3.31
C1s	291.77	284.49	279.42	21544.56	1.24	34219.47	0.43	55.73
N1s	404.97	400.08	395.72	1674.7	1.96	4275.89	0.03	4.31
O1s	538.87	530.47	526.22	8238	1.47	18049.81	0.09	11.1
F1s	692.37	685.93	681.87	8966.11	1.68	17623.93	0.06	8.13

Figure S8. X-ray photoelectron spectroscopy (XPS) of **2d-NP**. The binding energy peaks of Ag3d are 368.47 and 374.47 eV.

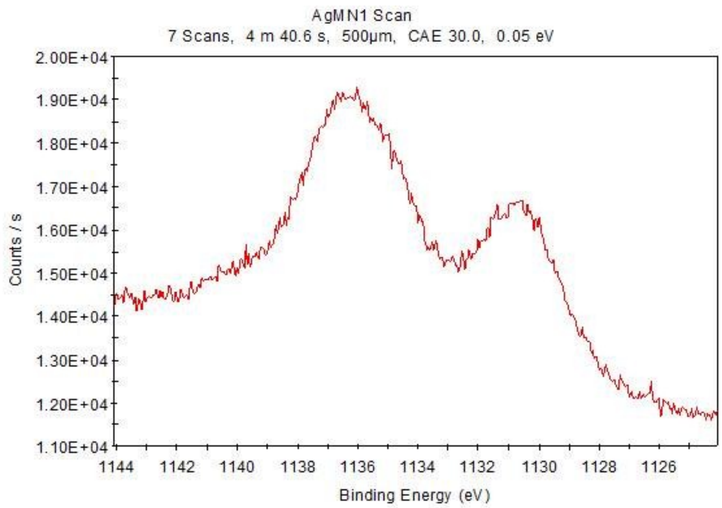

Figure S9. Auger electron spectroscopy (AES) of **2d-NP**. The binding energy peaks of Ag are 1130.57 and 1136.52 eV.

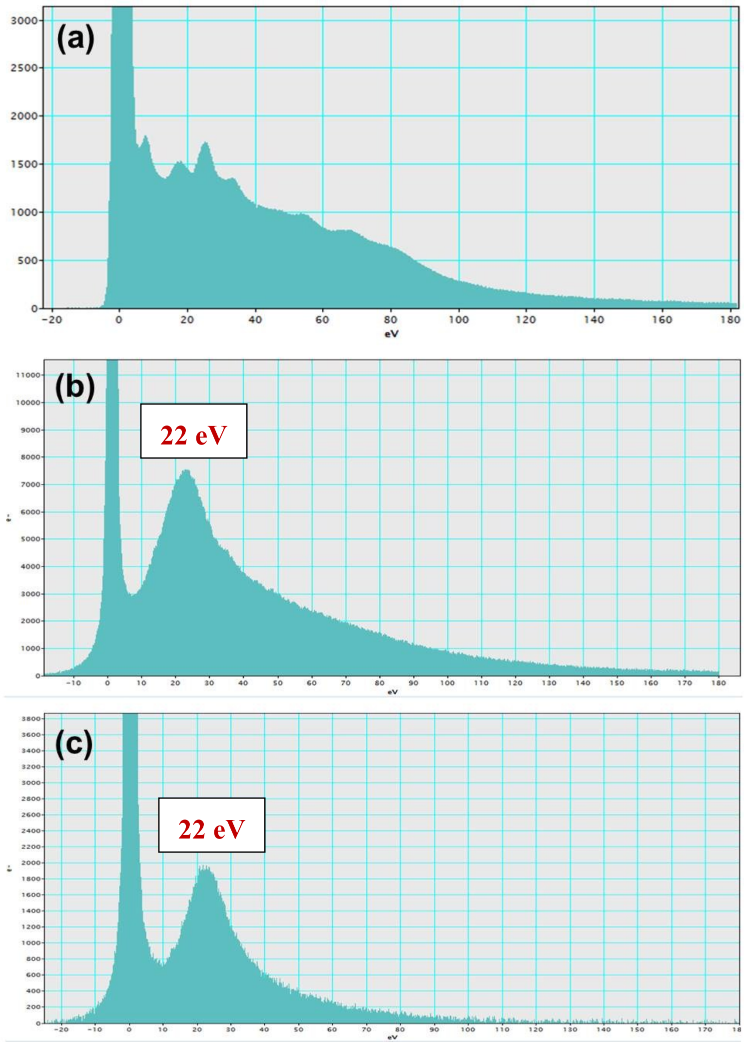

Figure S10. Electron energy loss spectroscopy (EELS) of (a) metallic Ag, (b) Ag_2S NPs, (c) **2d-NP**.

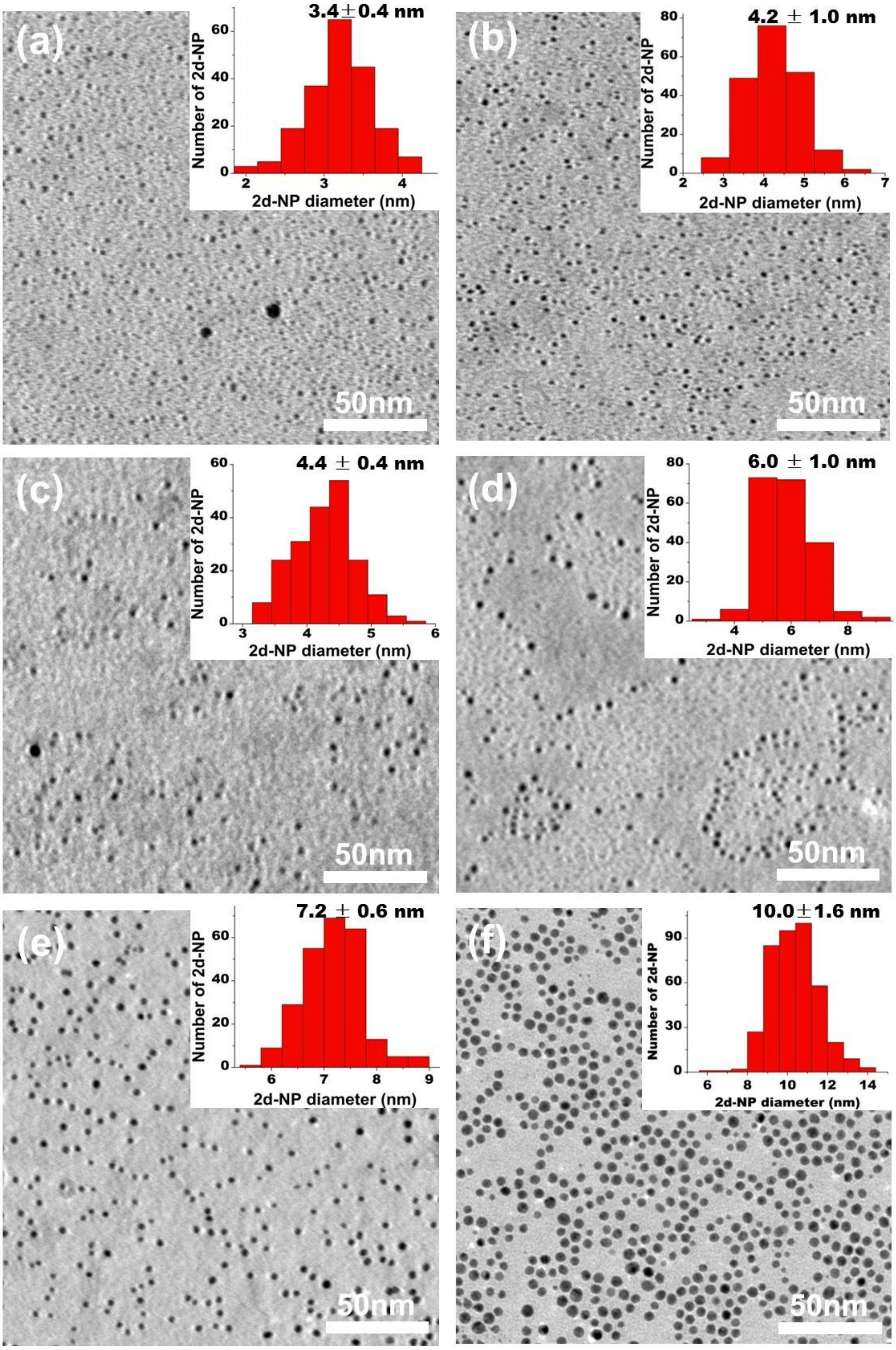

Figure S11. TEM images of differently sized **2d-NP**. The concentration of **2d** is (a) 0.8 g/L, 0.5 mL; (b) 0.8 g/L, 1.0 mL; (c) 0.8 g/L, 1.5 mL; (d) 0.8 g/L, 2.0 mL; (e) 0.8 g/L, 3.0 mL and (f) 0.8 g/L, 3.5 mL.

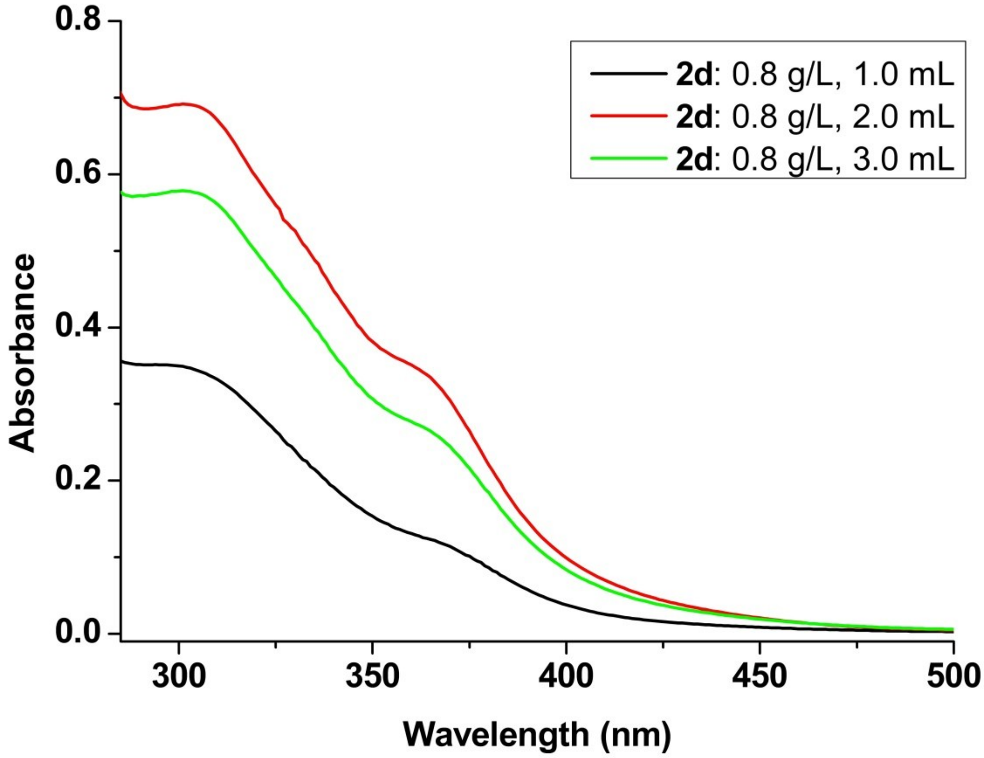

Figure S12. UV-vis absorption spectra of differently sized **2d-NP**. The two absorption peaks are 300 and 362 nm.

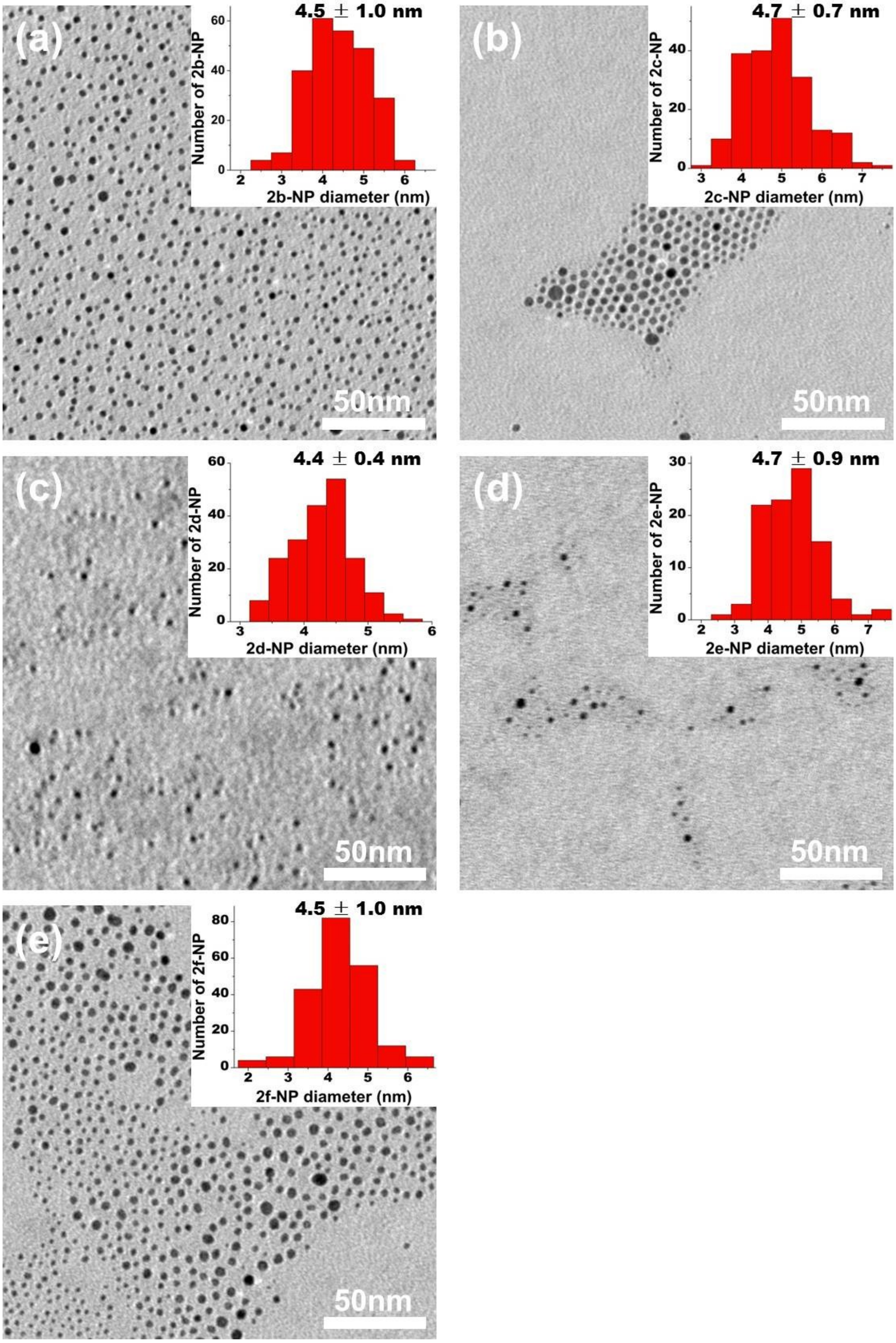

Figure S13. TEM of samples **2b-f-NP** derived from the same concentrated Py[6]-protected silver clusters with variable alkyl chain lengths from n-octyl to n-hexadecyl.

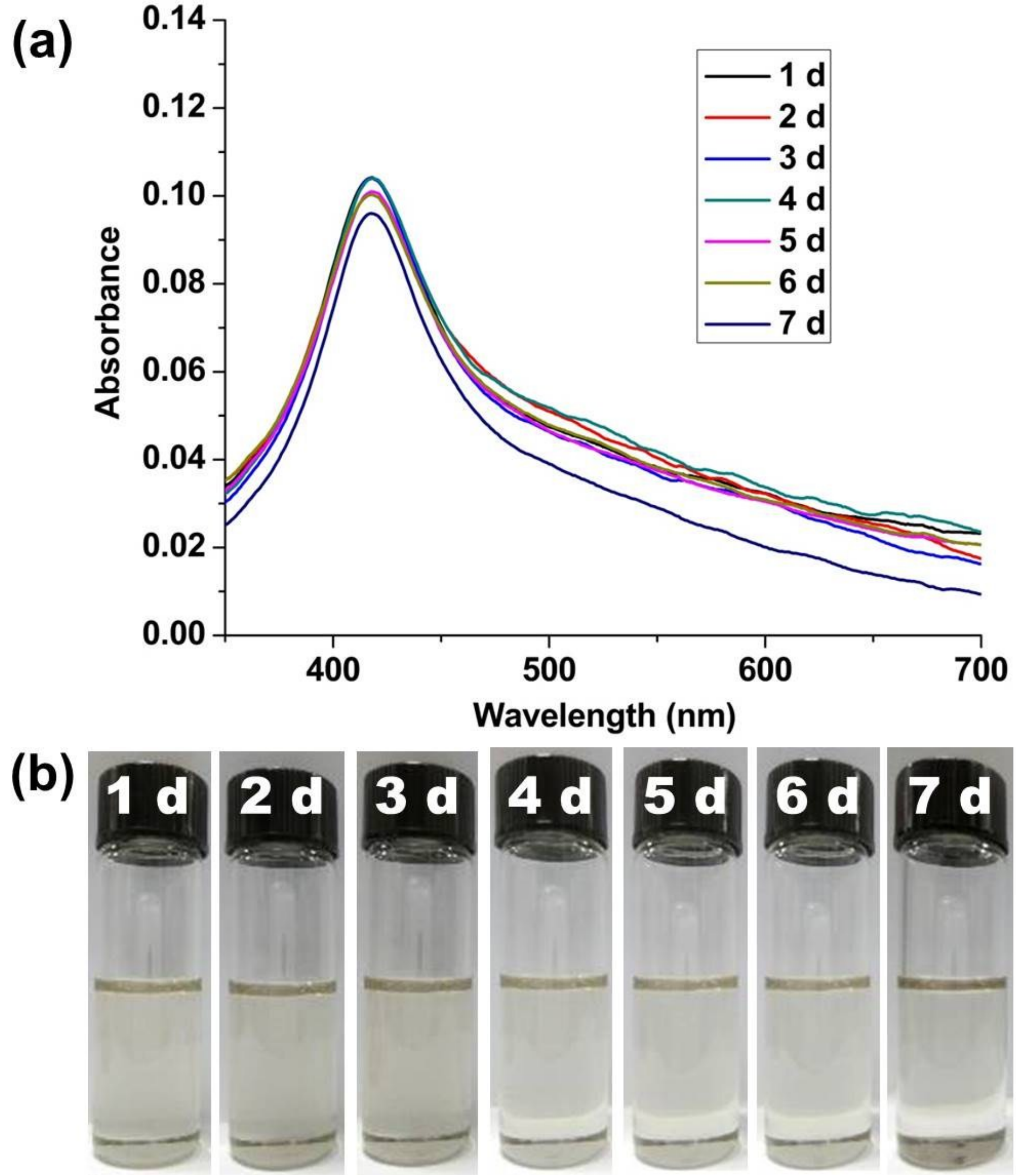

Figure S14. Monitoring the variation of (a) UV-vis spectra, and (b) photographs of **2d-Ag-NC** within one week to evaluate the stability of alkynyl-protected silver nanoclusters.

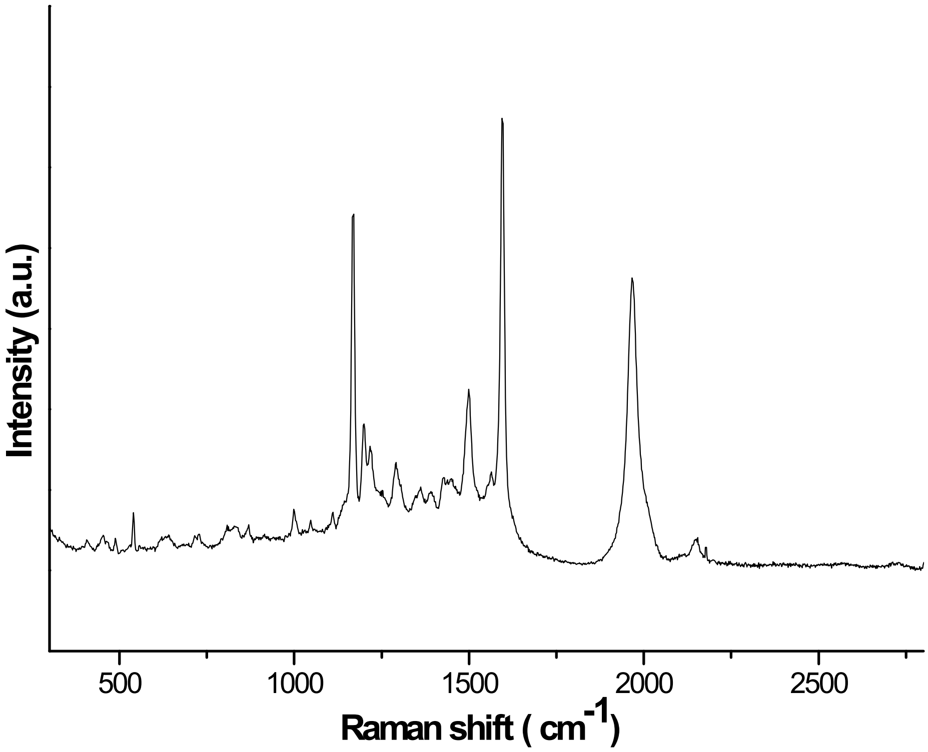

Figure S15. Raman spectrum of **2d-Ag-NC**. The Raman shift of C≡C is 1970 cm^{-1}.

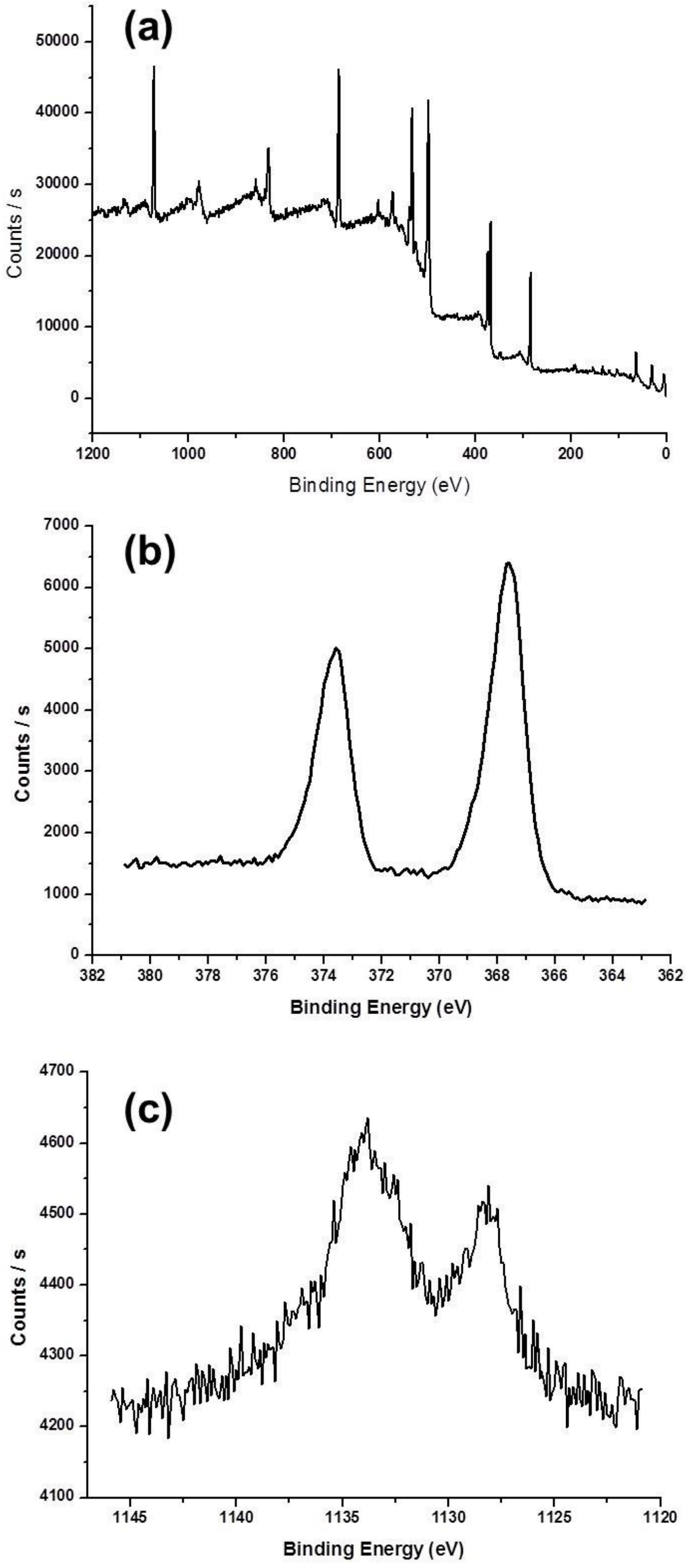

Figure S16. (a, b) X-ray photoelectron and (c) Auger electron spectroscopies of **2d-Ag-NC**. The binding energy peaks of Ag3d in XPS are 367.59 and 373.59 eV. In AES, the peaks are 1128.09 and 1133.79 eV.

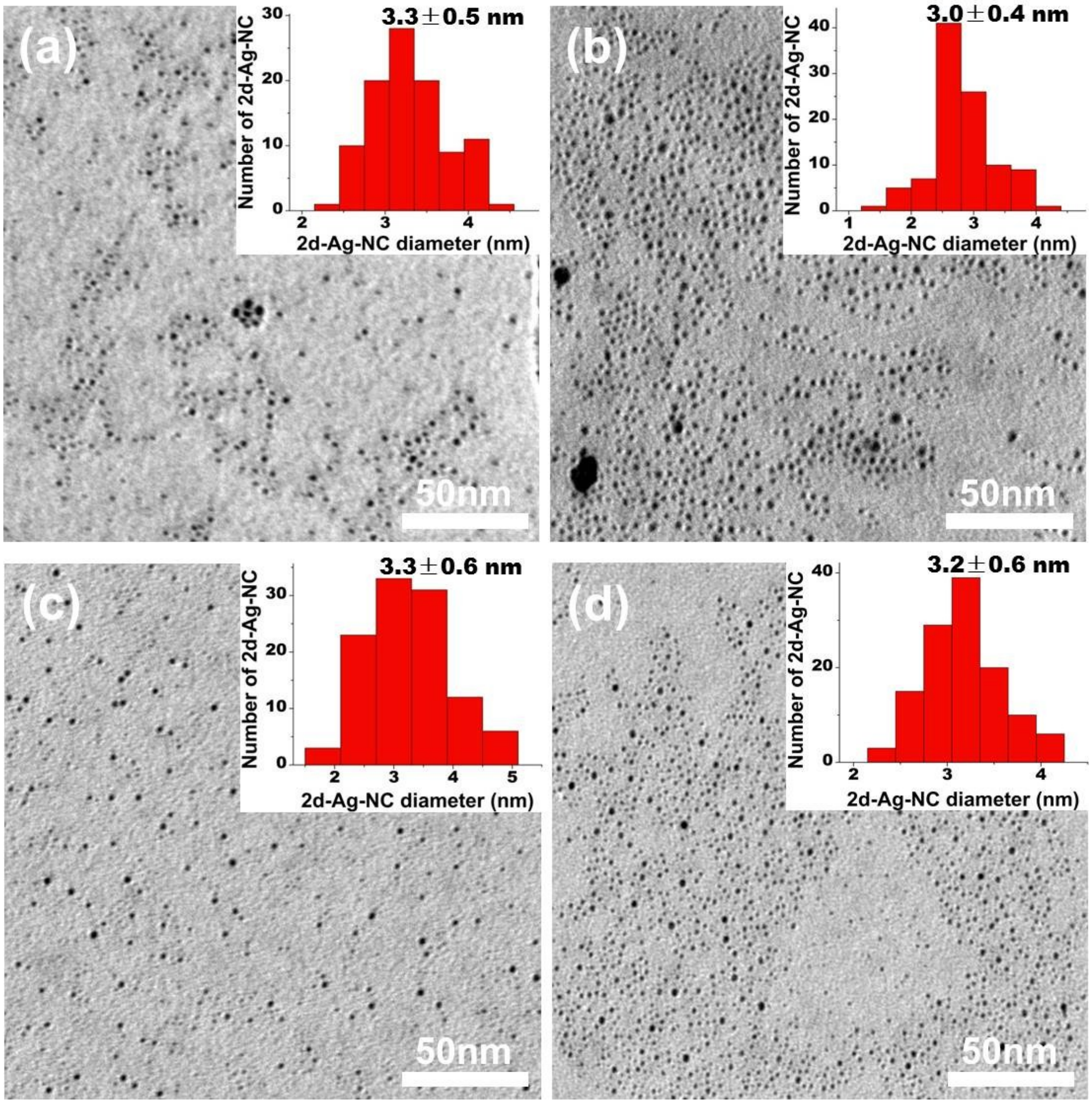

Figure S17. TEM images of **2d-Ag-NC**. The concentration of **2d** is (a) 0.8 g/L, 1.0 mL; (b) 0.8 g/L, 2.0 mL; (c) 0.8 g/L, 3.0 mL and (d) 0.8 g/L, 3.5 mL.